

DESIGN METHODOLOGY AND CHARACTERISTICS ANALYSIS OF HIGH-ORDER MULTI-SEGMENT DEFORMED ECCENTRIC NON-CIRCULAR GEAR

Huacheng Zhao^{1,2}, Jianneng Chen¹, Gaohuan Xu²

¹Faculty of Mechanical Engineering, Zhejiang Sci-Tech University, China

²School of Mechanical and Automotive Engineering,
Zhejiang University of Water Resource and Electric Power, China

Abstract. *A novel gear mechanism named high-order multi-segment deformed eccentric non-circular gear was proposed for achieving the unification of non-circular gears with typical-form pitch curve and non-circular gears with free-form pitch curve. The transmission mechanism of the high-order multi-segment deformed eccentric non-circular gear was analyzed, and the unified mathematical expression of eccentric gears was established. The non-circular gears with free-form pitch curve could be constructed based on the proposed high-order multi-segment deformed eccentric non-circular gear by changing the parameters. Moreover, the transmission characteristics were discussed, such as the transmission ratio relationship, convexity distinguished conditions, curvature radius of pitch curve. The visual design and simulation software and generation software of tooth profile for non-circular gears are compiled based on MATLAB, and was verified with the example. This novelty gear was applied to the drive mechanism of the metering pump. The mathematical model of non-circular gear-crank slider mechanism is established and the 3D model and virtual prototype experiment of the mechanism are accomplished. The application showed that the high-order multi-segment deformed eccentric non-circular gears were feasible in practice.*

Key words: *Concavity, Convexity, Eccentric gear, Free pitch curve, High-order, Multi-segment, Drive mechanism, Metering pump*

1. INTRODUCTION

Gears belong to the group of most effective mechanical power transmission components. They are characterized by very high efficiency, reliability, compact design, ease of finding

Received: February 27, 2023 / Accepted May 30, 2023

Corresponding author: Huacheng Zhao
School of Mechanical and Automotive Engineering, Zhejiang University of Water Resource and Electric power,
Hangzhou, 310018, China
E-mail: zhaohc@zjweu.edu.cn

a way to fit in specific applications – to name but a few properties. Many researchers devoted their work to investigate different aspects of gears, such as their optimization [1], health monitoring and diagnostics [2], thermal loadings [3], specific applications [4], wear resistance improvement [5], etc. This paper considers non-circular gears.

Non-circular gears can be accurately designed for intended movements to achieve periodic non-uniform transmission. Due to their precise transmission and ease of balance, non-circular gears are widely applied in agricultural machinery, packaging machinery, pumps, and light industry machinery [6-9]. According to the basic law of gear meshing, the pitch curves of a pair of gears with variable transmission ratios are no longer circular curves. The pitch curves of non-circular gears mainly include typical-form pitch curve and free-form pitch curve.

Free-form pitch curve cannot be clearly expressed with a mathematical function but often as a segmental curve. A method for constructing the N -lobe non-circular gear satisfying a specified displacement law with Bézier curve and B-spline curve was presented by Riaza et al. [10]. Medvecká-Beňová [11] presented a design of pitch curves for a given set of parameters and described how to apply an eccentric elliptical gear with a continuously changing transmission gear ratio to optimize the pitch curves of non-circular gears. Fanghella [12] presented a new method for designing non-circular gears under a given law of motion based on a mixed symbolic-numeric approach. Li et al. [13] proposed to express non-circular gear pitch curves by means of numerical points instead of any function, for the purpose of fitting complex form pitch curves. In the attempt of analyzing the generation process of noncircular gears, Vasie and Andrei [14] introduced the Gielis super-shape equation to fit the pitch curve. This method was focused on convex-concave gear generation.

Gears with typical-form pitch curve can be expressed with typical mathematical models, such as elliptical gear, eccentric gear and Fourier non-circular gear. Elliptical gear is the most commonly used gear and has been extensively studied. Subsequently, high-order elliptical gears and deformed elliptical gears are proposed through adjusting the numbers of cycle of pitch curves [15-18]. Additionally, non-circular gears with typical-form pitch curve have also been vigorously explored and investigated in the design and transmission characteristics, including eccentric noncircular gears, Fourier noncircular gears, and Pascal spiral gears, further to enrich gear transmission form [19-21].

Eccentric noncircular gears have also been widely studied because of a simple pitch curve and convenient processing. In the studies on eccentric circular gears, the high-order eccentric gears have been obtained by keeping the polar radius of eccentric circular gear unchanged and reducing the polar angle by an integral multiple. The high-order eccentric gears can get different numbers of blade with different orders, which can realize multiple periodic transmission ratio [22]. Chen et al. [23] have proposed deformed eccentric noncircular gear by changing the transmission ratio into two asymmetric segments and deduced the equation of pitch curve, which is applied to the weft insertion mechanism.

The varying forms of pitch curves make it impossible to obtain non-circular gears with free pitch curve, thereby increasing great difficulty of standardized design of non-circular gears. Non-circular gears with typical-form pitch curve have less flexible pitch curves and limited changes in transmission ratios and, hence, they are unable to satisfy a much broader range of transmission requirements. To unify these two kinds of non-circular gears and standardize the design, a high-order multi-segment deformed eccentric non-circular gear is

put forward to construct non-circular gears with free pitch curve. The novel gear divides the pitch curve into more than three segments in a cycle and makes the shape of the pitch curve more changeable and enriching the transmission types of non-circular gear.

The advantages of periodic multistage variable transmission of high-order multi-segment deformed eccentric non-circular gear can better meet the requirements of variable transmission ratios, which can be used as a driver for the seal mechanisms of horizontal pillow packing machine, differential pump, etc. The gear pair can also be combined with other mechanisms. The high-order multi-segment deformed eccentric non-circular gear pair and crank slider mechanism can be connected to form a combined mechanism, which can greatly improve the stability of the slider speed and reduce the impact vibration. By adjusting the parameters of the combined mechanism, specific movement output can be obtained, which can be applied to metering pump, hay baler mechanism and pulsating blood flow generator.

In this article, section 2 puts forward transmission mechanism of high-order multi-segment deformed eccentric non-circular gear and a mathematical model of that is built. Section 3 analyzes the transmission characteristics, such as transmission ratio, curvature radius and convexity distinguished conditions. In section 4, the visual design and simulation software is developed and a design case is illustrated to verify the feasibility of the proposed gears. Then, an application is given, followed by conclusions.

2. DESIGN OF HIGH-ORDER MULTI-SEGMENT DEFORMED ECCENTRIC NON-CIRCULAR GEAR

2.1 Transmission Mechanism of Multi-segment Deformed Eccentric Non-circular Gear

In general eccentric non-circular gear transmission, the driving gear 1 is an eccentric circular gear and the driven gear 2 is a non-circular gear which conjugates with the eccentric circular gear, as indicated in Fig. 1. Based on the analysis of equations of pitch curve of general eccentric non-circular gears, we proposed a high-order deformed eccentric non-circular gears [23]. The equations of pitch curve are as follows.

$$\left\{ \begin{array}{l} r_{11} = R(\sqrt{1 - k^2 \sin^2(n_1 m_{11} \varphi_1)} - k \cos(n_1 m_{11} \varphi_1)) \quad \text{for } (0 \leq \varphi_1 \leq \frac{\pi}{n_1 m_{11}}) \\ r_{12} = R(\sqrt{1 - k^2 \sin^2(n_1 m_{12} (\frac{2\pi}{n_1} - \varphi_1))} - k \cos(n_1 m_{12} (\frac{2\pi}{n_1} - \varphi_1))) \quad \text{for } (\frac{\pi}{n_1 m_{11}} \leq \varphi_1 \leq \frac{2\pi}{n_1}) \end{array} \right. \quad (1)$$

where r_{11} , r_{12} are the polar radii of the eccentric gear for two segments, R is radius of the eccentric gear, k is the eccentricity ratio ($k=e/R$, e is the eccentricity of eccentric gear), φ_1 is the polar angle of the eccentric gear, n_1 is the order of the eccentric gear, m_{11} , m_{12} are the deformation coefficients.

The pitch curve expressed in Eq. (1) for the high-order deformed eccentric non-circular gear presents two asymmetrical segments in each cycle. Thus, the number of deformed segments is small, and the adjustment range of transmission ratio is limited. The pitch curve is still a typical form and cannot replace non-circular gear with free pitch curve.

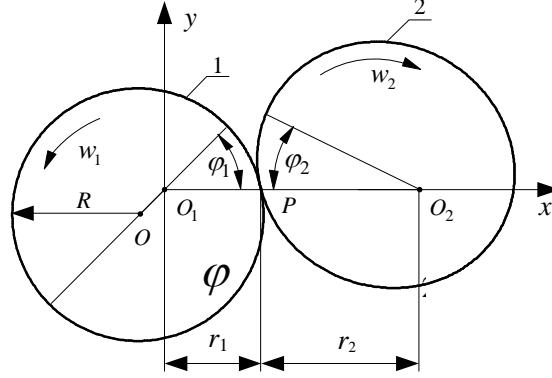


Fig. 1 Pitch curves of eccentric non-circular gears

For the possibility of changing pitch curve forms and obtaining a wider range of transmission ratio, the pitch curve is divided into N (more than three) segments eccentric circle with different deformation coefficients. In this manner, a multi-segment deformed eccentric non-circular gear can be obtained. Every segment is a deformed eccentric circle. Eq. (2) is the equation of the pitch curve of multi-segment deformed eccentric non-circular gear.

$$\left\{ \begin{array}{l} r_{11} = R(\sqrt{1-k^2 \sin^2(m_{11}\varphi_1)} - k \cos(m_{11}\varphi_1)) \text{ for } (0 \leq \varphi_1 \leq \frac{2\pi}{Nm_{11}}) \\ r_{12} = R(\sqrt{1-k^2 \sin^2(m_{12}(\varphi_1 - \frac{2\pi}{Nm_{11}}) + \frac{2\pi}{N})} - k \cos(m_{12}(\varphi_1 - \frac{2\pi}{Nm_{11}}) + \frac{2\pi}{N})) \\ \text{for } (\frac{2\pi}{Nm_{11}} \leq \varphi_1 \leq \frac{2\pi}{Nm_{11}} + \frac{2\pi}{Nm_{12}}) \\ r_{ij} = R(\sqrt{1-k^2 \sin^2(m_{ij}(\varphi_1 - 2\pi \sum_{k=1}^{j-1} \frac{1}{Nm_{1k}}) + \frac{2(j-1)\pi}{N})} \\ - k \cos(m_{ij}(\varphi_1 - 2\pi \sum_{k=1}^{j-1} \frac{1}{Nm_{1k}}) + \frac{2(j-1)\pi}{N})) \text{ for } (\sum_{k=1}^{j-1} \frac{2\pi}{Nm_{1k}} \leq \varphi_1 \leq \sum_{k=1}^j \frac{2\pi}{Nm_{1k}}) \end{array} \right. \quad (2)$$

where r_{1j} is the radius of the eccentric gear for segment j , j is the sequence number of the segment, while $j=1,2,3\dots N$, N is the number of segments, m_{1j} is the deformation coefficient for segment j , $m_{1j} > 1/N$ and must satisfy the following equation:

$$\sum_{k=1}^{N_1} \frac{1}{m_{1k}} = N \quad (3)$$

According to Eq. (2), for $\varphi_1 = 2\pi \sum_{k=1}^{j-1} \frac{1}{Nm_{1k}}$,

$$r_j = r_{i(j-1)} = R(\sqrt{1-k^2 \sin^2 [2(j-1)\pi/N]} - k \cos [2(j-1)\pi/N]) \quad (4)$$

For $\varphi_1 = 0$ and $\varphi_1 = 2\pi$,

$$r_{1N} = r_{11} = R(1-k) = R-e \quad (5)$$

Hence, the pitch curve of a multi-segment deformed eccentric non-circular gear formed by Eq. (2) is continuous at $\varphi_1 = 2\pi \sum_{k=1}^{j-1} \frac{1}{Nm_{1k}}$, $\varphi_1 = 0$ and $\varphi_1 = 2\pi$. Therefore, it is a continuous closed curve.

2.2 Transmission Mechanism of High-order Multi-segment Deformed Eccentric Non-circular Gear

As shown in Fig. 2, combined with the formation principles of the pitch curves for a high-order eccentric gear and a multi-segment deformed eccentric gear, the pitch curve of the high-order eccentric gear is divided in each cycle into N ($N \geq 3$) segments to form a high-order multi-segment deformed eccentric non-circular gear.

The equation of the pitch curve of the driving gear is given as follows:

$$\left. \begin{aligned} r_{1i1} &= R(\sqrt{1-k^2 \sin^2 (n_1 m_{11} \varphi_1)} - k \cos (n_1 m_{11} \varphi_1)) \quad \text{for } (0 \leq \varphi_1 \leq \frac{2\pi}{N n_1 m_{11}}) \\ r_{1i2} &= R(\sqrt{1-k^2 \sin^2 (n_1 m_{12} (\varphi_1 - \frac{2\pi}{N n_1 m_{11}}) + \frac{2\pi}{N})} - k \cos (n_1 m_{12} (\varphi_1 - \frac{2\pi}{N n_1 m_{11}}) + \frac{2\pi}{N})) \\ &\quad \text{for } (\frac{2\pi}{N n_1 m_{11}} \leq \varphi_1 \leq \frac{2\pi}{N n_1 m_{11}} + \frac{2\pi}{N n_1 m_{12}}) \\ r_{1ij} &= R(\sqrt{1-k^2 \sin^2 (n_1 m_{1j} (\varphi_1 - 2\pi \sum_{k=1}^{j-1} \frac{1}{N n_1 m_{1k}}) + \frac{2(j-1)\pi}{N})} \\ &\quad - k \cos (n_1 m_{1j} (\varphi_1 - 2\pi \sum_{k=1}^{j-1} \frac{1}{N n_1 m_{1k}}) + \frac{2(j-1)\pi}{N})) \quad \text{for } (\sum_{k=1}^{j-1} \frac{2\pi}{N n_1 m_{1k}} \leq \varphi_1 \leq \sum_{k=1}^j \frac{2\pi}{N n_1 m_{1k}}) \end{aligned} \right\} \quad (6)$$

where r_{1ij} is the radius of the eccentric gear for segment j of cycle i , while i is the cycle number of the driving gear and $i = 1, 2, 3, \dots, n_1$.

According to Eq. (6), in any cycle i , for $\varphi_1 = 2\pi \sum_{k=1}^{j-1} \frac{1}{N n_1 m_{1k}}$:

$$r_{ij} = r_{i(j-1)} = R(\sqrt{1-k^2 \sin^2 [2(j-1)\pi/N]} - k \cos [2(j-1)\pi/N]) \quad (7)$$

Eq. (7) shows that all the segments of the deformed pitch curve within each cycle are connected.

At the junction of any adjacent cycles, for $\varphi_1 = 0$ or $\varphi_1 = 2\pi \sum_{k=1}^j \frac{1}{N n_1 m_{(i-1)k}}$,

$$r_{i1} = r_{1(i-1)N} = R(1-k) = R-e \quad (8)$$

Eq. (8) shows that all the segments of the deformed pitch curve are connected.

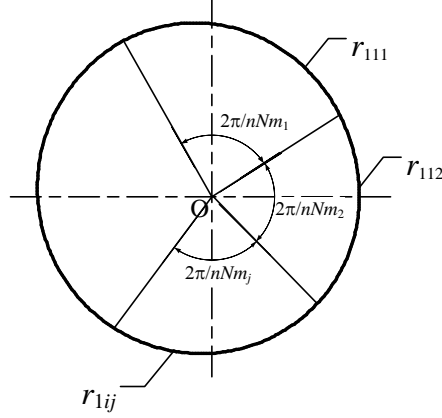


Fig. 2 Schematic diagram of pitch curve

Therefore, the pitch curve of a non-circular gear, which is given by Eq. (6), is a continuous closed curve. And within a cycle of 2π , each segment of the pitch curve is connected.

According to the basic requirement of gear meshing, the variation of angular displacements of the driving gear and the driven gear should be accomplished in the same period. This can be expressed by the following relationship [24]:

$$\varphi_2 = \int_0^{\varphi_1} \frac{1}{i_{12}} d\varphi_1 = \int_0^{\varphi_1} \frac{r_1}{a-r_1} d\varphi_1 \quad (9)$$

Consequently, the closure condition of the pitch curves of a high-order multi-segment deformed eccentric non-circular gear is established as:

$$\begin{aligned} \frac{2\pi}{n_2} &= \int_0^{2\pi} \frac{1}{i_{12}} d\varphi_1 = \int_0^{\frac{\pi}{Nn_1m_1}} \frac{r_{1i1}}{a-r_{1i1}} d\varphi_1 + \sum_{j=2}^N \int_{2\pi}^{2\pi} \sum_{k=1}^{j-1} \frac{1}{Nn_1m_k} \frac{r_{1ij}}{a-r_{1ij}} d\varphi_1 \\ &= \int_0^{\frac{\pi}{Nn_1m_1}} \frac{\sqrt{R^2 - e^2 \sin^2(n_1 m_1 \varphi_1)} - e \cos(n_1 m_1 \varphi_1)}{a - (\sqrt{R^2 - e^2 \sin^2(n_1 m_1 \varphi_1)} - e \cos(n_1 m_1 \varphi_1))} d\varphi_1 + \\ &\quad \sum_{j=2}^N \int_{2\pi}^{2\pi} \sum_{k=1}^{j-1} \frac{1}{Nn_1m_k} \frac{\sqrt{R^2 - e^2 \sin^2(n_1 m_j (\varphi_1 - \sum_{k=1}^{j-1} \frac{2\pi}{Nn_1m_k}) + \frac{2(j-1)\pi}{N})} - e \cos(n_1 m_j (\varphi_1 - \sum_{k=1}^{j-1} \frac{2\pi}{Nn_1m_k}) + \frac{2(j-1)\pi}{N})}{a - (\sqrt{R^2 - e^2 \sin^2(n_1 m_j (\varphi_1 - \sum_{k=1}^{j-1} \frac{2\pi}{Nn_1m_k}) + \frac{2(j-1)\pi}{N})} - e \cos(n_1 m_j (\varphi_1 - \sum_{k=1}^{j-1} \frac{2\pi}{Nn_1m_k}) + \frac{2(j-1)\pi}{N}))} d\varphi_1 \end{aligned} \quad (10)$$

where n_2 is the order of the driven gear.

The centre distance a is solved based on Eq. (10). The centre distance a is obviously controlled by the following design parameters: R , e , n_1 , N and m_{ij} . The process of solving the centre distance is shown below:

(1) Searching the unimodal interval where the centre distance is located with the Advance-Retreat Method;

(2) Determining the centre distance with the Golden Section Method.

From Eq. (6) and Eq. (10), the equations of radius and polar angle of the driven gear are written as Eq. (11) and Eq. (12), respectively:

$$\begin{cases} r_{2i1} = a - R(\sqrt{1 - k^2 \sin^2(n_1 m_{11} \varphi_1)} - k \cos(n_1 m_{11} \varphi_1)) & \text{for } (0 \leq \varphi_1 \leq \frac{2\pi}{N n_1 m_{11}}) \\ r_{2ij} = a - R(\sqrt{1 - k^2 \sin^2(n_1 m_{1j} (\varphi_1 - 2\pi \sum_{k=1}^{j-1} \frac{1}{N n_1 m_{1k}}) + \frac{2(j-1)\pi}{N})} - k \cos(n_1 m_{1j} (\varphi_1 - 2\pi \sum_{k=1}^{j-1} \frac{1}{N n_1 m_{1k}}) + \frac{2(j-1)\pi}{N})) & \text{for } (\sum_{k=1}^{j-1} \frac{2\pi}{N n_1 m_{1k}} \leq \varphi_1 \leq \sum_{k=1}^j \frac{2\pi}{N n_1 m_{1k}}) \end{cases} \quad (11)$$

$$\varphi_2 = \begin{cases} \int_0^{\varphi_1} \frac{\sqrt{R^2 - e^2 \sin^2(n_1 m_{11} \varphi_1)} - e \cos(n_1 m_{11} \varphi_1)}{a - (\sqrt{R^2 - e^2 \sin^2(n_1 m_{11} \varphi_1)} - e \cos(n_1 m_{11} \varphi_1))} d\varphi_1 & \text{for } (0 \leq \varphi_1 \leq \frac{2\pi}{N n_1 m_{11}}) \\ \int_0^{\frac{2\pi}{N n_1 m_{11}}} \frac{\sqrt{R^2 - e^2 \sin^2(n_1 m_{11} \varphi_1)} - e \cos(n_1 m_{11} \varphi_1)}{a - (\sqrt{R^2 - e^2 \sin^2(n_1 m_{11} \varphi_1)} - e \cos(n_1 m_{11} \varphi_1))} d\varphi_1 + \\ \int_{\sum_{k=1}^{N-1} \frac{2\pi}{N n_1 m_{1k}}}^{\varphi_1} \frac{\sqrt{R^2 - e^2 \sin^2(n_1 m_{1j} (\varphi_1 - \sum_{k=1}^{j-1} \frac{2\pi}{N n_1 m_{1k}}) + \frac{2(j-1)\pi}{N})} - e \cos(n_1 m_{1j} (\varphi_1 - \sum_{k=1}^{j-1} \frac{2\pi}{N n_1 m_{1k}}) + \frac{2(j-1)\pi}{N})}{a - (\sqrt{R^2 - e^2 \sin^2(n_1 m_{1j} (\varphi_1 - \sum_{k=1}^{j-1} \frac{2\pi}{N n_1 m_{1k}}) + \frac{2(j-1)\pi}{N})} - e \cos(n_1 m_{1j} (\varphi_1 - \sum_{k=1}^{j-1} \frac{2\pi}{N n_1 m_{1k}}) + \frac{2(j-1)\pi}{N}))} d\varphi_1 & \text{for } (\sum_{k=1}^j \frac{2\pi}{N n_1 m_{1k}} \leq \varphi_1 \leq \sum_{k=1}^j \frac{2\pi}{N n_1 m_{1k}}) \end{cases} \quad (12)$$

Clearly, the driven gear, which conjugates with the driving gear, is a non-circular gear with n_2 -order and N -segment. For different numbers of segments N , the following is valid:

(1) if $N=1$, $m_{1j}=1$, $n_1=n_2=1$, the driving gear 1 is a general eccentric circular gear and driven gear 2 is a non-circular gear, which conjugates with driving gear 1.

(2) if $N=2$, the driving gear 1 is a high-order deformed eccentric non-circular gear as shown in Eq. (1), and the driven gear 2 is a high-order deformed non-circular gear, which conjugates with the driving gear 1.

(3) if $N \geq 3$, driving gear 1 is essentially a non-circular gear with n_1 -order and N -segment and the driven gear 2 is non-circular gear with n_2 -order and N -segment which conjugates with the driving gear 1.

Therefore, the high-order multi-segment deformed eccentric non-circular gears proposed in the paper are more general and unified in theory, and more extensively used in practice, as high-order eccentric non-circular gear and multi-segment deformed eccentric non-circular gear are covered. Through changing the design parameters such as R , e , n_1 , n_2 ,

N and m_{ij} , the non-circular gears with a free-form pitch curve could be composed by the high-order multi-segment deformed eccentric non-circular gear.

Fig. 3 shows two examples of pitch curves, with different order and segment numbers, while the other parameters are the same: (a) $n_1=1, n_2=3, N=2$ and (b) $n_1=3, n_2=2, N=3$.

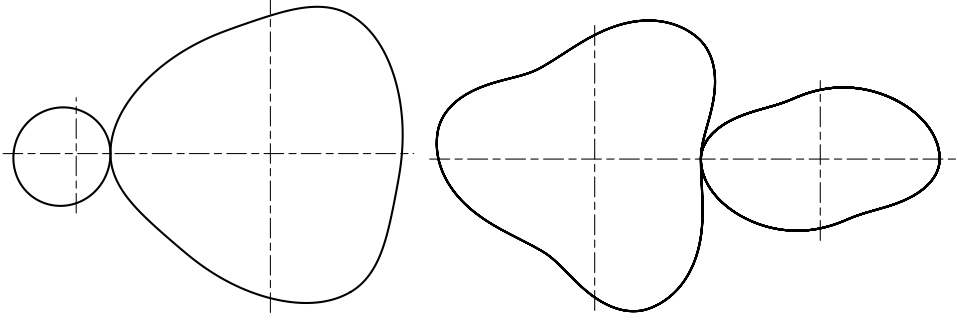


Fig. 3 Cases of the pitch curves: left: $n_1=1, n_2=3, N=3$; right: $n_1=3, n_2=3, N=3$

3. ANALYSIS OF TRANSMISSION CHARACTERISTIC

3.1 Transmission Ratio

According to the definition of the transmission ratio, the transmission ratio of high-order multi-segment deformed eccentric non-circular gear is expressed as follows. To simplify

the analysis, let $\alpha = n_1 m_{1j} (\varphi_1 - \sum_{k=1}^{j-1} \frac{2\pi}{N n_1 m_{1k}}) + \frac{2(j-1)\pi}{N}$.

$$i_{12} = \frac{\omega_1}{\omega_2} = \frac{r_2}{r_1} = \frac{a-r_1}{r_1} = \frac{a-R(\sqrt{1-k_1^2 \sin^2 \alpha} - k_1 \cos \alpha)}{R(\sqrt{1-k_1^2 \sin^2 \alpha} - k_1 \cos \alpha)} \quad \text{for } (\frac{2(j-1)\pi}{N} \leq \alpha \leq \frac{2\pi}{N}) \quad (13)$$

For $n_1 m_{1j} (\varphi_1 - \sum_{k=1}^{j-1} \frac{2\pi}{N n_1 m_{1k}}) + \frac{2(j-1)\pi}{N} \in [0, 2\pi]$, when $\varphi_1 = \frac{2(1-j)\pi/N}{n_1 m_{1j}} + \sum_{k=1}^{j-1} \frac{2\pi}{N n_1 m_{1k}}$, i_{12} is at the minimum:

$$i_{12\min} = \frac{a-(R+e)}{R+e} \quad (14)$$

For $\varphi_1 = \frac{\pi+2(1-j)\pi/N}{n_1 m_{1j}} + \sum_{k=1}^{j-1} \frac{2\pi}{N n_1 m_{1k}}$, i_{12} is at the maximum:

$$i_{12\max} = \frac{a-(R-e)}{R-e} \quad (15)$$

Therefore, according to Eq. (15) and (16), the maximum and minimum transmission ratios are designed to determine the range of i_{12} .

3.2 Concavity and Convexity

The pitch curves of high-order multi-segment deformed eccentric circular non-circular gear may be concave. In order to drive stably and conveniently, the concavity and convexity of the pitch curves shall be verified.

The curvature radius of pitch curve of high-order multi-segment deformed eccentric non-circular gear is obtained based on the knowledge of differential geometry, hence:

$$\rho(\varphi) = \frac{\left[r^2(\varphi) + \left(\frac{dr}{d\varphi} \right)^2 \right]^{\frac{3}{2}}}{r^2(\varphi) + 2 \left(\frac{dr}{d\varphi} \right)^2 - r(\varphi) \frac{d^2r}{d\varphi^2}} \quad (16)$$

As for the driving gear, the derivations of the first segment of the pitch curve in each cycle are calculated from Eq. (6).

$$\frac{dr_1}{d\varphi_1} = \frac{dr_{i1}}{d\varphi_1} = -\frac{e^2 n_1 m_{11} \sin(2n_1 m_{11} \varphi_1)}{2\sqrt{R^2 - e^2 \sin^2(n_1 m_{11} \varphi_1)}} + e n_1 m_{11} \sin(n_1 m_{11} \varphi_1) \quad (17)$$

$$\frac{d^2r_1}{d\varphi_1^2} = \frac{d^2r_{i1}}{d\varphi_1^2} = e n_1^2 m_{11}^2 \cos(n_1 m_{11} \varphi_1) - \frac{e^2 n_1^2 m_{11}^2 \cos(2n_1 m_{11} \varphi_1)}{\sqrt{R^2 - e^2 \sin^2(n_1 m_{11} \varphi_1)}} - \frac{e^4 n_1^2 m_{11}^2 \sin^2(2n_1 m_{11} \varphi_1)}{4\sqrt{(R^2 - e^2 \sin^2(n_1 m_{11} \varphi_1))^3}} \quad (18)$$

The curvature radius of the first segment curve could be solved by substituting Eqs. (17) and (18) into Eq. (16).

When the curvature radius meets the following condition, the pitch curve is convex:

$$\rho(\varphi) \geq 0 \quad (19)$$

For $n_1 m_{11} \varphi_1 = 0$, the curvature radius of the first segment is at its minimum:

$$\rho_{i1} = \frac{(R - e)^2}{R - e[1 + n_1^2 m_{11}^2 (1 - k)]} \quad (20)$$

From Eq. (14), it can be seen that the numerator is greater than zero. If $R - e[1 + n_1^2 m_{11}^2 (1 - k)] > 0$, the pitch curve of this segment becomes convex, so the convexity distinguished condition of this segment can be simplified as:

$$(n_1^2 m_{11}^2 k - 1)(k - 1) > 0 \quad (21)$$

In this case, the convexity distinguishing conditions is expressed below:

$$k < \frac{1}{n_1^2 m_{11}^2} \quad (22)$$

For the driving gear, the convexity distinguished condition in each segment is:

$$k < \min \left\{ \frac{1}{n_1^2 m_{1j}^2} \right\} \quad (23)$$

The curvature radius of the driven gear can also be solved using Eq. (16), but the derivation is complicated. In this paper, it is calculated by Euler-Savary formula [24], which is expressed as:

$$\frac{1}{\rho_{p1}} + \frac{1}{\rho_{p2}} = \left(\frac{1}{r_1} + \frac{1}{r_2} \right) \sin \mu_1 \quad (24)$$

where $\sin \mu_1 = \sqrt{R^2 - e^2 \sin^2(n_1 m_{11} \varphi_1)} / \rho_1$.

After simplification and calculation, the convexity distinguishing condition of the pitch curve for each segment is expressed below:

$$\left. \begin{aligned} k < \min \left\{ \frac{1}{n_1^2 m_{1j}^2} \right\} \\ (1+k)^2 - ae / R^2 \geq 0 \end{aligned} \right\} \quad (25)$$

The non-circular gears can be processed by hobbing when they meet the conditions given by Eqs. (23) and (25).

4. DESIGN CASE AND DISCUSSION

4.1 Compiling of design software

In order to better analyze their transmission characteristics, the visual design and simulation software and the generation software of the tooth profile for non-circular gears are developed using MATLAB based on the equations of the pitch curve of high-order multi-segment deformed eccentric non-circular gear, which have been established in section 2, as showed in Figs. 4 and 5.

Based on the mechanism parameters (R , e , n_1 , n_2 , N and m_{ij}), the software can determine the center distance, the transmission ratio and the curvature radius, as well as the kinematic curves of the driven gear, including the displacement, velocity and acceleration. The developed software also enables simulation of the pitch curves development.

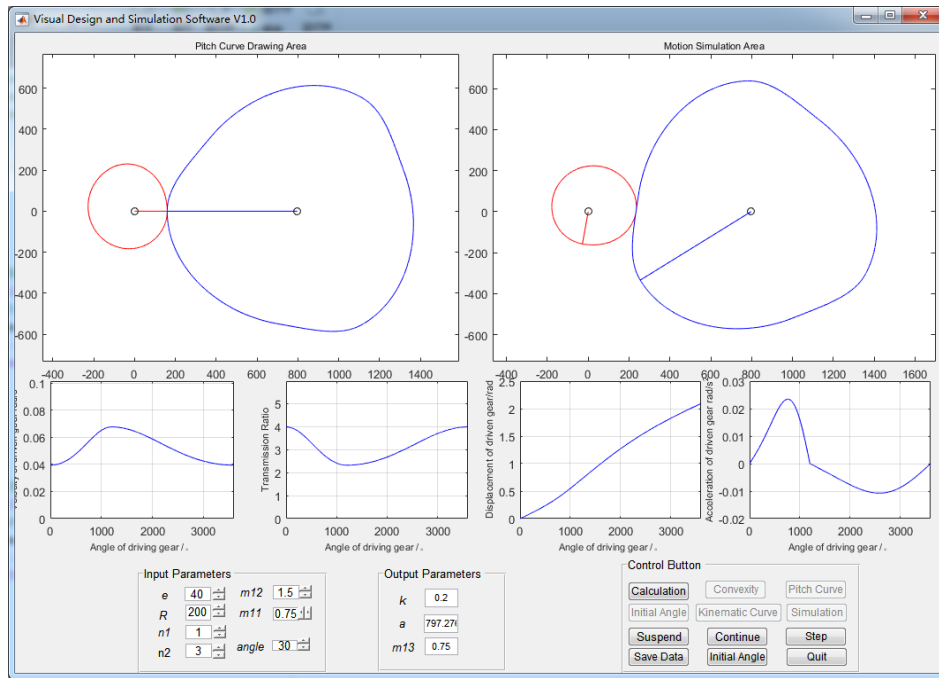


Fig. 4 Software of visual design and simulation

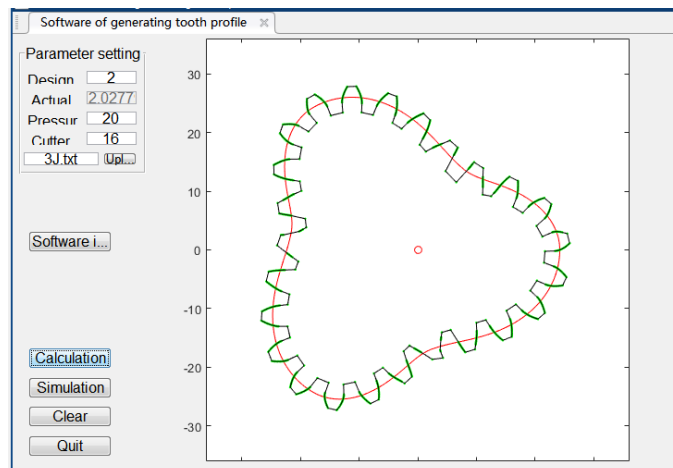


Fig. 5 Software of generating tooth profile

4.2 Design case and Discussion

A gear pair meets the conditions as follows: $R = 100\text{mm}$, $e = 10\text{mm}$, $n_1 = 3$, $n_2 = 4$, $N = 3$, $m_{11} = 1.5$, and $m_{11} = 0.75$. The visual design and simulation software is utilized to determine the following parameters: $a = 233.67\text{mm}$, $k = 0.1$ and $m_{13} = 1$.

For the gear pair, the pitch curves and tooth profile are depicted in Figs. 6 and 7 respectively. The driving gear 1 is a three-order and three-segment deformed eccentric non-circular gear, while the driven gear 2 is a four-order and three-segment non-circular gear.

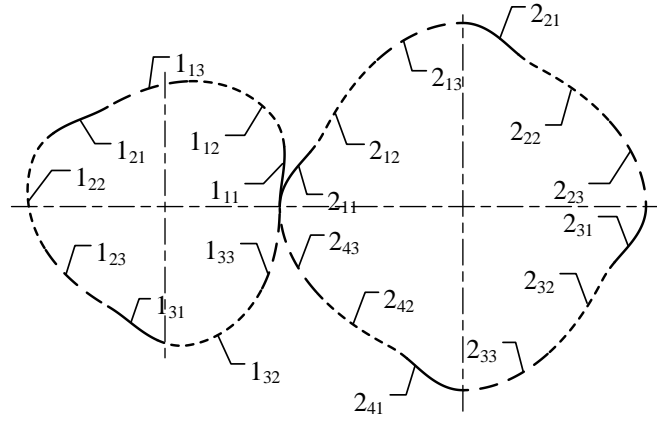


Fig. 6 Pitch Curves of Gears

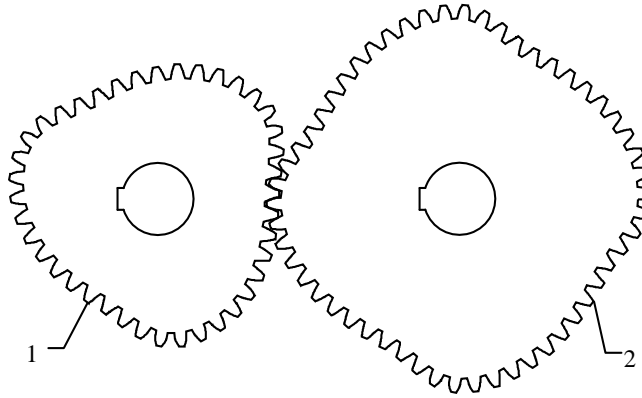


Fig. 7 Tooth Profiles of Gears

The curves of transmission ratio and curvature radius are obtained using the developed visual design and simulation software, Fig. 8 shows that the transmission ratio is continuous and divided into three asymmetrical segments in each cycle.

As for the pitch curve of the driving gear, the convexity distinguishing conditions of each segment in the cycle are $k \leq 0.049$, $k \leq 0.198$ and $k \leq 0.111$, respectively. In this example, $k = 0.1$, so the pitch curve is concave in first segment of each cycle for the driving gear and the curvature radius is negative, as shown in Fig. 9. The curvature radius is not continuous at the connection points. Similarly, the pitch curve is concave in first segment of each cycle for the driven gear. Specifically, the pitch curve suddenly changes at the segmentation points, where the pitch curve transforms from convex to concave, or transforms from concave to convex.

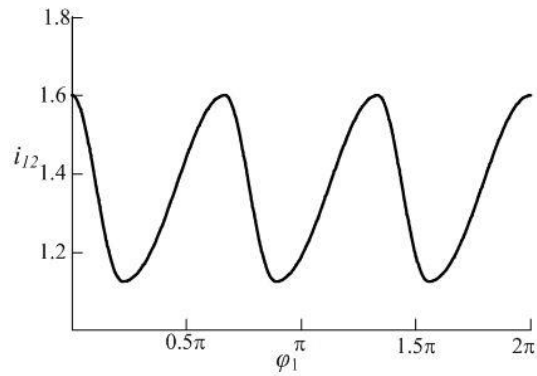


Fig. 8 Curve of Transmission Ratio

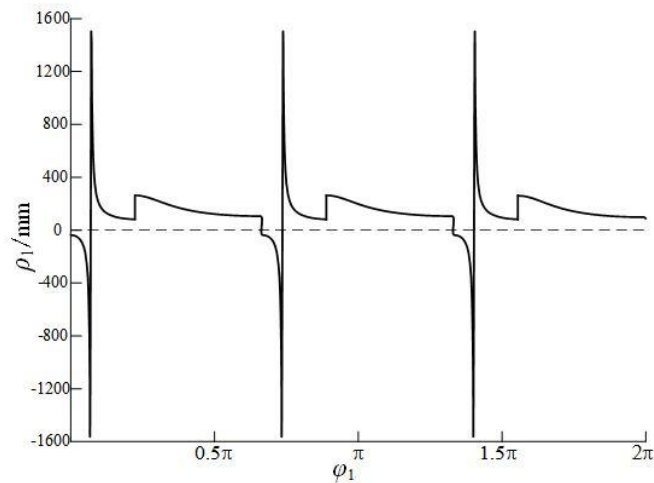


Fig. 9 Curvature radius of driving gear

5. APPLICATION

In this paper, this novel gear is applied to the drive mechanism of the metering pump. The metering pump is a special positive displacement pump with the ability to vary capacity as the process conditions require. It is capable of pumping a wide range of liquids including acids, bases, corrosives or viscous liquids. The pumping action is generated by a reciprocating piston. The function of the drive mechanism is to transform the rotary motion of the driver into reciprocating movement [25-26].

When the crank slider mechanism is used as the drive mechanism of metering pump, the curve of the output speed of slider is similar with a sine wave. The speed of the slider changes nonlinearly in the transmission process, which makes the slider gain acceleration and increases its reciprocating inertial force. It causes vibration and noise of the pump and aggravate the impact and wear between the components.

In order to stabilize the output speed of the crank slider mechanism and reduce the impact vibration of the pump, a non-circular gear-crank slider mechanism is proposed as the drive mechanism of metering pump. Figure 10 shows the schematic diagram of non-circular gear-crank slider drive mechanism of the metering pump.

The motor drives the driving gear to rotate with a uniform speed and drives the driven non-circular gear to rotate at a non-uniform speed. Crank O_2A is fixed on the driven non-circular gear and the crank follows the driven gear at the same speed. The motion is transferred to the piston through the transmission of crank slider mechanism and realizes the reciprocating motion.

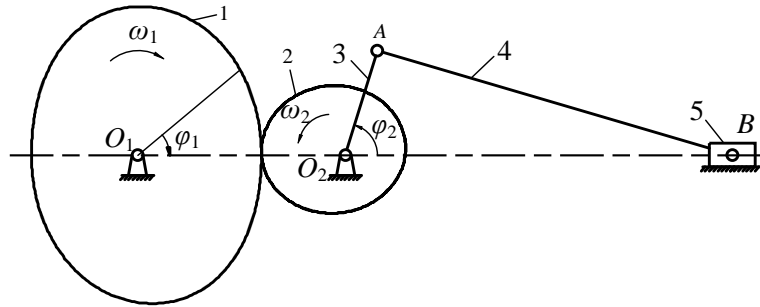


Fig. 10 Diagram of non-circular gear-crank slider mechanism: 1. Driving gear, 2. Driven gear, 3. Crank 4. Connecting rod, 5. Slider

5.1 Mathematical model of non-circular gear-crank slider mechanism

Fig.11 is the schematic diagram of the crank slider mechanism. The crank is fixed on the driven gear of the non-circular gear pair, so the angular displacement (angular velocity) of the crank is equal to the angular displacement (angular velocity) of the driven gear. The slider displacement can be expressed as:

$$s = \sqrt{l_2^2 - l_1^2 \sin^2 \varphi_2} + l_1 \cos \varphi_2 - (l_2 - l_1) \quad (26)$$

where s is the displacement of slider, l_1 is the length of crank, l_2 is the length of connecting rod, φ_2 the angular displacement of the driven gear.

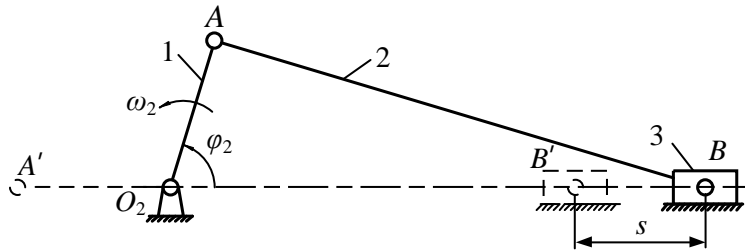


Fig. 11 Diagram of crank slider: 1. Crank 2. Connecting rod, 3. Slider

Calculate the derivative of Eq. (27) to obtain the velocity of the slider:

$$v = \frac{ds}{dt} = -l_1 \omega_2 \left(\sin \varphi_2 + \frac{l_1 \sin(2\varphi_2)/l_2}{2\sqrt{1-(l_1^2 \sin^2 \varphi_2)}} \right) \quad (27)$$

The output speed of the crank can be obtained using Eq. (13), so that:

$$\omega = \omega_2 = \frac{\omega_1}{i_{12}} \quad (28)$$

From Eqs. (27) and (28), it can be obtained that the velocity of the slider in the combined mechanism is:

$$v = -\frac{l_1 \omega_1}{i_{12}} \left(\sin \varphi_2 + \frac{l_1 \sin(2\varphi_2)/l_2}{2\sqrt{1-(l_1^2 \sin^2 \varphi_2)}} \right) \quad (29)$$

To simplify the analysis, Eq. (29) can be rewritten as:

$$\frac{v}{\omega_1} = -\frac{l_1}{i_{12}} \left(\sin \varphi_2 + \frac{\varepsilon \sin(2\varphi_2)}{2\sqrt{1-(\varepsilon^2 \sin^2 \varphi_2)}} \right) \quad (30)$$

where $\varepsilon = l_1/l_2$ is the length ratio of the crank and connecting rod.

When the driving gear rotates at a constant speed, the variation law of the output speed of the combined mechanism can be obtained from Eq. (30).

By adjusting the parameters of the high-order multi-segment deformed eccentric non-circular gear and the length ratio of crank and connecting rod, the speed of the stroke and return section of the combined mechanism is approximately uniform, which can reduce the reciprocating inertia force generated by the transmission system, the vibration and impact of the instantaneous flow on the pump. Fig.12 shows the comparison of the velocity curves of a non-circular gear-crank slider mechanism and a crank slider mechanism.

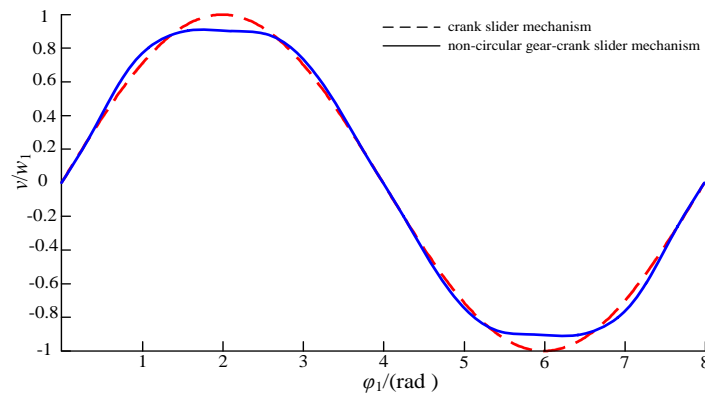


Fig. 12 Comparison of velocity curves of two transmission mechanisms

5.2 Virtual Simulation

According to the mechanism parameters obtained from the analysis, the 3D model and virtual assembly of the mechanism are accomplished using Solidworks software. The 3D-model is shown in Fig. 13. It was imported into the ADAMS software and constraints were added together with the drive for a virtual prototype experiment. Kinematics simulation of this mechanism was conducted. The velocity curve of the slider obtained by the virtual experiment is shown in Fig. 14.

It can be found that the velocity curves obtained by theoretical calculations are nearly the same as that of the virtual experiment. This fact can be seen as their mutual verification. The main reason why the two curves are not completely coincident is that deformation is included in the virtual experiment as each part is considered to be deformable by adding their material properties.

But some fluctuations in the velocity curve of the slider may still be observed. The reason for this is to be sought in some interstices between kinematics pairs in the transmission route, which results in the decrease of the transmission accuracy.

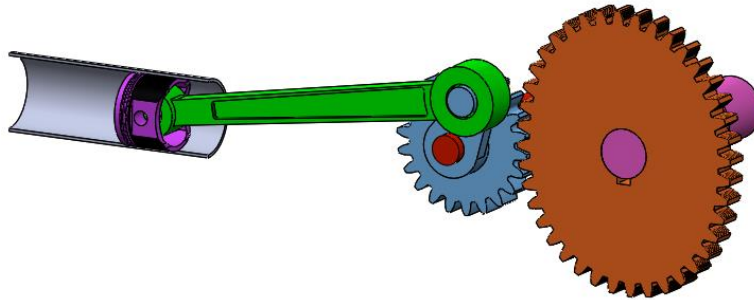


Fig. 13 3D model of the combined mechanism

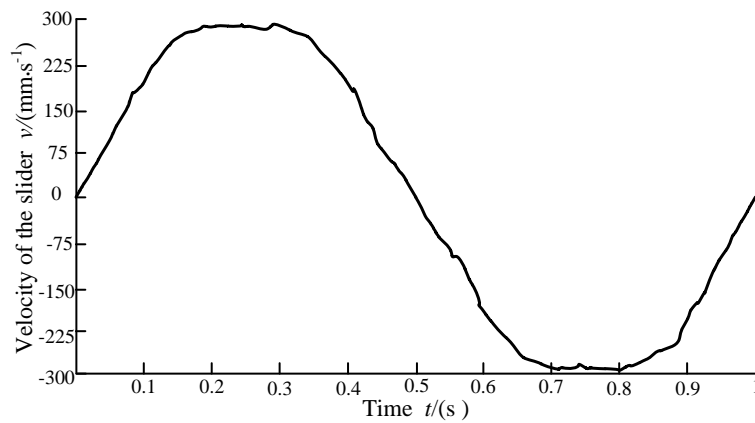


Fig. 14 The curve of velocity of slider got by simulation

6. CONCLUSIONS

The design method for high-order multi-segment deformed eccentric non-circular gear is proposed upon analysis of the high-order eccentric non-circular gear and the multi-segment deformed eccentric non-circular gear. Unified mathematical expressions of eccentric non-circular gears are obtained, which expands their applicability. The method proposed in this paper has wide potential applicability to other non-circular gears with a typical-form pitch curve, such as elliptical gears, Fourier gears and Pascal spiral gears.

The pitch curve shape of the high-order multi-segment deformed eccentric non-circular gear could be adjusted by changing some design parameters such as R , e , n_1 , n_2 , N and m_{ij} . Hence, the pitch curves are easily adjustable (free-form). Consequently, the non-circular gears with a free-form pitch curve can be obtained from high-order multi-segment deformed eccentric non-circular gear by changing the design parameters, which provides a theoretical basis for unifying these two kinds of non-circular gears. The transmission ratio and design of non-circular gears can be flexibly adjusted so that the requirements of precision transmission are met in order to improve transmission performance.

The visual design and simulation software are compiled using MATLAB and based on the proposed mathematical expressions. The verification was done using an example. This novel gear was applied to the drive mechanism of the metering pump. Comparing the results of theoretical analysis and the virtual prototype experiment, the velocity curve of the slider obtained by simulation is in a good agreement with the ideal velocity curve. This shows that the proposed non-circular gear-crank-slider mechanism can meet the functional requirements of the metering pump, and verifies the feasibility of the designed mechanism. The design example illustrates that the high-order multi-segment deformed eccentric non-circular gear mesh correctly and can be utilized in practice.

Acknowledgement: *The paper is a part of the research done within the project of the National Natural Science Foundation of China (Grant No. 51975536), the Natural Science Foundation of Zhejiang Province (Grant No. LY21E050002) and the Science Research Project of Department of Education of Zhejiang Province (Grant No. Y201941866).*

REFERENCES

1. Stefanović-Marinović, J., Vrcan, Ž., Troha, S., Milovančević, M., 2022, *Optimization of two-speed planetary gearbox with brakes on single shafts*, Reports in Mechanical Engineering, 3(1), pp. 94-107.
2. Kundu, P., Darpe, A.K., Kulkarni, M.S., 2021, *A review on diagnostic and prognostic approaches for gears*, Structural Health Monitoring, 20(5), pp. 2853-2893.
3. Miltenović, A., Tica, M., Banić, M., Miltenović, Đ., 2020, *Prediction of temperature distribution in the worm gear meshing*, Facta Universitatis-Series Mechanical Engineering, 18(2), pp. 329-339.
4. Tica, M., Vrcan, Ž., Troha, S., Marinkovic, D., 2023, *Reversible planetary gearsets controlled by two brakes, for internal combustion railway vehicle transmission applications*, Acta Polytechnica Hungarica, 20(1), pp. 95-108.
5. Mao, K., Greenwood, D., Ramakrishnan, R., Goodship, V., Shrouti, C., Chetwynd, D., Langlois, P., 2019, *The wear resistance improvement of fibre reinforced polymer composite gears*, Wear, 426-427, part B, pp. 1033-1039.
6. Litvin, F.L., Gonzalez-Perez, I., Fuentes, A., Hayasaka, K., 2008, *Design and investigation of gear drives with non-circular gears applied for speed variation and generation of functions*, Computer Methods in Applied Mechanics and Engineering, 197(45-48), pp. 3783-3802.

7. Petre A., Dragos M., Catalin A., 2012, *A gear with translational wheel for a variable transmission ratio and applications to steering box*, Mechanism and Machine Theory, 52, pp. 267–276.
8. Maláková, S., Urbanský, M., Fedorko, G., Molnár, V., Sivak, S., 2021, *Design of Geometrical Parameters and Kinematical Characteristics of a Non-circular Gear Transmission for Given Parameters*, Applied Sciences, 11(3), 1000.
9. Kujawski, M., Krawiec, P., 2011, *Analysis of generation capabilities of noncircular Cogbelt pulleys on the example of a gear with an elliptical pitch line*, Journal of Manufacturing Science and Engineering, 133(5), 051006.
10. Rianza, H.F.Q., Foix, S.C., Nebot, L.J., 2007, *The synthesis of a N-lobe noncircular gear using Bézier and B-spline nonparametric curve on the design of its displacement law*, Journal of Mechanical Design, 129(9), pp. 982-985.
11. Medvecká-Benová, S., 2018, *Designing pitch curves of non-circular gears*, Scientific Journal of Silesian University of Technology, Series Transport, 99, pp. 105–114.
12. Fanghella, P., 2005, *Kinematic synthesis and design of non-circular gears through a symbolic-numeric modeling approach*, Proc. of the ASME 2005 International Design Engineering Technical Conferences and Computers and Information in Engineering Conference, Long Beach, California, USA, pp. 781-789.
13. Li, G., Ying, K.Y., Zheng F.J., Gu, J.B., Xu, Z.W., 2014, *Design and experiment of noncircular gears transplanting mechanism based on pitch curve with nonfunction expression*, Transactions of the Chinese Society of Agricultural Engineering, 30(23), pp. 10-16.
14. Vasie, M., Andrei, L., 2012, *Design and generation of noncircular gears with convex-concave pitch curves*, The Annals of Dunarea de Jos University of Galati, Fascicle V, Technologies in Machine Building, pp. 55-60.
15. Mehmet, Y., 2021, *Design, manufacturing and operational analysis of elliptical gears*, International Journal of Precision Engineering and Manufacturing, 22, pp. 1441–1451.
16. Figliolini, G., Angeles, J., 2005, *Synthesis of the base curves for N-lobed elliptical gears*, Journal of Mechanical Design, 127(5), pp. 997–1005.
17. Prikhodko, A., 2020, *Experimental kinematic analysis of an intermittent motion planetary mechanism with elliptical gears*, Journal of Measurements in Engineering, 8(3), pp. 122-131.
18. Han, J., Liu, Y.Y., Li, D.Z., Xia, L., 2016, *External high-order multisegment modified elliptical helical gears and design procedure of their gear pairs*, Proceedings of the institution of mechanical engineers Part C-Journal of Mechanical Engineering Science, 230(16), pp. 2929–2939.
19. Xu, G.H., Chen, J.N., Zhao, H.C., 2018, *Numerical calculation and experiment of coupled dynamics of the differential velocity vane pump driven by the hybrid higher-order fourier non-circular gears*, Journal of Thermal Science, 27(3), pp. 285-293.
20. Starzhinsky, V.E., Mardosevich, E.I., Basinyuk, V.L., Ossipenko, S.A., 2007, *Gearmotors with a planetary eccentric gear train for service and mechatronic systems*, ASME International Design Engineering Technical Conferences and Computers and Information in Engineering Conference, Las Vegas, Nevada, USA, pp. 1053-1059.
21. Liu, Y.P., Wang, P., Xian, X.L., Zhang, S.Y., 2015, *Design of the tooth profile of Pascal curve gear*, Journal of Mechanical Transmission, 39(03), pp. 50-52.
22. Figliolini, G., Migliozzi, P., Engineersasme, A., Engineersasme, A., 2004, *Synthesis of the pitch cones of N-lobed elliptical bevel gears*, ASME Design Engineering Technical Conferences, Cassino, Italy, 43-03043.
23. Chen, J.N., Zhao, H.C., Wang, Y., Xu, G.H., Zhou, M., 2013, *Kinematic modeling and characteristic analysis of eccentric conjugate non-circular gear & crank-rocker & gears train weft insertion mechanism*, Journal of Donghua University(Eng. Ed.), 30(01), pp. 15-20.
24. Park, Y., Wei, S., Park, H., 2021, *Effect of the variable gear mesh model in dynamic simulation of a drive train in the wind turbine*, Engineering Review, 41(2), pp.113-124.
25. Giovanni, M. Paolo, P., 2001, *Diaphragm design improvement for a metering pump*, Engineering Failure Analysis, 8(1), pp. 1-13.
26. Borstell, D., 2005, *Benefits of the rotary diaphragm pump*, Medical Device Technology, 16(2), pp. 16-18.